JOURNAL OF VIROLOGY, Oct. 2007, p. 11096–11105 Vol. 81, No. 20
0022-538X/07/$08.00+0 doi:10.1128/JVI.01249-07

A Rab-GAP TBC Domain Protein Binds Hepatitis C Virus NS5A and Mediates Viral Replication▽

Ella H. Sklan,[1] Kirk Staschke,[2] Tina M. Oakes,[2] Menashe Elazar,[1] Mark Winters,[1] Benjamin Aroeti,[1]† Tsafi Danieli,[1]† and Jeffrey S. Glenn[1,3]*

Division of Gastroenterology and Hepatology, Stanford University School of Medicine,[1] and Veterans Administration Medical Center,[3] Palo Alto, California, and Lilly Research Laboratories, Indianapolis, Indiana[2]

Received 8 June 2007/Accepted 16 July 2007

Hepatitis C virus (HCV) is an important cause of liver disease worldwide. Current therapies are inadequate for most patients. Using a two-hybrid screen, we isolated a novel cellular binding partner interacting with the N terminus of HCV nonstructural protein NS5A. This partner contains a TBC Rab-GAP (GTPase-activating protein) homology domain found in all known Rab-activating proteins. As the first described interaction between such a Rab-GAP and a viral protein, this finding suggests a new mechanism whereby viruses may subvert host cell machinery for mediating the endocytosis, trafficking, and sorting of their own proteins. Moreover, depleting the expression of this partner severely impairs HCV RNA replication with no obvious effect on cell viability. These results suggest that pharmacologic disruption of this NS5A-interacting partner can be contemplated as a potential new antiviral strategy against a pathogen affecting nearly 3% of the world's population.

HCV is a positive single-stranded RNA virus whose 9.6-kb genome encodes an ~3,000-amino-acid polyprotein that is proteolytically processed into structural proteins (components of the mature virus) and nonstructural proteins (involved in replicating the viral genome) (15, 20). The nonstructural protein 5A (NS5A) is part of the intracellular membrane-associated viral replication complex (15). Mutations in NS5A affect the rate of HCV replication (3). NS5A has generated considerable interest because of a postulated role in determining the response to interferon (21). A variety of host proteins have been reported to interact with NS5A, although for most their precise relevance in the HCV life cycle awaits definition.

Like that of all positive-strand RNA viruses, HCV replication occurs in intimate association with specific intracellular membrane structures, which for HCV has been termed the membranous web (8). What host machinery is exploited to establish these sites of viral replication is unknown. Rab GTPases are small GTP-binding proteins that regulate vesicular-membrane-trafficking pathways, behaving as membrane-associated molecular switches (22). Rab proteins have been previously implicated in the life cycles of various enveloped viruses and are utilized by these viruses for endocytosis, trafficking, and sorting of their proteins (see, for example, Vonderheit and Helenius [33]). Because NS5A has been implicated in the membrane-associated replication of HCV (10), we hypothesized that among the host cell factors that associate with NS5A might be components of host cell membrane-trafficking machinery. To test this hypothesis, we used the full-length NS5A from genotype 1b as bait to screen a human liver cDNA prey library in a GAL4-based yeast two-hybrid screen. We have identified a TBC protein family member, TBC1D20, as a binding partner of HCV NS5A. TBC domain proteins contain an ~200-amino-acid motif initially identified in the TRE2/BUB2/CDC16 genes (25). Like all TBC family members, TBC1D20 contains a Rab-GTPase-activating protein (GAP) homology domain required for regulating the activity of Rab proteins. Depletion of TBC1D20 expression severely impaired HCV replication and inhibited new infection. We propose a model in which TBC1D20 and the Rab-GTPase(s) under its control help mediate the establishment of the HCV replication complex.

MATERIALS AND METHODS

Plasmids. Standard recombinant-DNA technology was used to construct and purify all plasmids. All regions that were amplified by PCR were analyzed by automated DNA sequencing. Plasmid DNAs were prepared from large-scale bacterial cultures and purified with a Maxiprep kit (Marligen Biosciences). Restriction enzymes were purchased from New England Biolabs. Yeast plasmids are described below. The Bart79I plasmid, which contains the HCV subgenomic replicon Bart79I, was described previously (9). To make pEF6-NS5A, full-length NS5A was amplified from Bart79I and inserted into pEF6 myc-His A (Invitrogen) with a stop codon at the end of NS5A and upstream of the sequences encoding the Myc and His tags.

The plasmid pCMV-Flag-TBC1D20 was made by cloning full-length TBC1D20 (GenBank accession no. NM_144628) obtained from the yeast two-hybrid-positive clone into the pcDNA3.1 vector (Invitrogen) with an N-terminal FLAG tag. The plasmids used for the in vitro translation reactions were pCMV-HA-TBC1D20, pCMV-NS5A-FLAG, and pCMV-NS5A mAH-FLAG. To make pCMV-HA-TBC1D20, full-length TBC1D20 was cloned into pcDNA3.1 with an N-terminal hemagglutinin (HA) tag. pCMV-NS5A-Flag was made by cloning NS5A from Bart79I into pcDNA3.1 with a C-terminal Flag tag. The amphipathic helix (AH) mutant (mAH) NS5A was previously described (10). Briefly, the hydrophobic face of the helix was disrupted by site-specific PCR mutagenesis. Three charged amino acids spaced at intervals along the predicted N-terminal α-helix were introduced so that no sustained hydrophobic patch remained (isoleucine-8, isoleucine-12, and phenylalanine-19 of NS5A were changed to aspartate, glutamate, and aspartate, respectively). To make pCMV-EGFP-TBC1D20, full-length TBC1D20 was cloned into pEGFP-C1 (Clontech) so that the C

* Corresponding author. Mailing address: Stanford University School of Medicine, CCSR 3115A, 269 Campus Drive, Palo Alto, CA 94305-5187. Phone: (650) 725-3373. Fax: (650) 723-3032. E-mail: jeffrey.glenn@stanford.edu.

† Present address: Alexander Silberman Institute of Life Sciences, Hebrew University of Jerusalem, Jerusalem, Israel.

▽ Published ahead of print on 8 August 2007.

terminus of green fluorescent protein (GFP) was fused in frame to the N terminus of TBC1D20. To make pCMV-NS5A-DsRed, full-length NS5A was amplified from Bart79I and cloned into pDsRed-N1 (Clontech). In this plasmid, the N terminus of DsRed was fused in frame to the C terminus of NS5A. Bart-HA was made by removal of amino acids 2209 to 2254 in Bart79I and insertion of a 21-amino-acid-encoding sequence (TACCCGTACGACGTACCGGACTACGC AGCGGCCGCATACCCGTACGACGTACCGGACTACGCA) corresponding to two HA tags flanking a NotI site by direct cloning into NS5A of Bart79I.

Yeast two-hybrid assays. A GAL4-based yeast two-hybrid screen (Matchmaker yeast two-hybrid system; Clontech, Palo Alto, CA) was used to screen for host cell-interacting partners of NS5A. Full-length NS5A from genotype 1b was cloned into the GAL binding domain (BD)-containing plasmid pGBKT7 (which supplies leucine) and screened against a human liver cDNA prey library fused to the GAL4 activation domain (AD) (whose vector supplies tryptophan) (Clontech). For screening, plasmids were transfected into competent AH109 cells (Clontech) according to the manufacturer's protocol. Growth on SD medium (Clontech) without tryptophan, leucine, histidine, and adenine was used as evidence that both an AD (Trp)- and a BD (Leu)-containing plasmid were present and that a functional interaction occurred (leading to the transcription of genes producing histidine and adenine). Out of 8.6×10^5 clones screened, we isolated 73 positive clones. DNA from these colonies was extracted, and library plasmids were isolated by transformation into *Escherichia coli* and ampicillin selection. The library insert DNA was sequenced and identified by comparison to the human genome database. To confirm the interactions, library plasmids were retransformed into yeast (*Saccharomyces cerevisiae*), together with plasmid pGBKT7-NS5A or with pGBKT7-Lamin C as a negative control. Protein partners that regrew in the presence of NS5A and did not grow with the lamin C control were chosen for further analysis. One of these, TBC1D20, was the result of a full-length clone isolated in the screen and is the subject of this report. The TBC1D20-NS5A interaction was further confirmed by switching the bait and prey plasmids (so that NS5A was fused to the AD and TBC1D20 was fused to the BD). Cotransfection of the NS5A bait plasmid (BD-NS5A), along with an empty prey plasmid (AD^-), or of the TBC1D20 prey plasmid (AD-TBC1D20) with an irrelevant bait (lamin C) plasmid (BD-Lam) did not yield growth on selective media, indicating that neither NS5A nor TBC1D20 alone could self-activate the system. Cotransfection of plasmids encoding lamin C (BD-Lam) and T antigen (AD-T Ag) served as a negative control, while the interaction between p53 (BD-P53) and T antigen (AD-T Ag) served as a positive control. All of the mutants for TBC1D20-NS5A interaction assays in yeast were prepared from the pGBK-NS5A plasmid described above and a full-length TBC1D20 clone inserted into pGADT7.

Immunoprecipitations (IPs). The TBC1D20-NS5A interaction was confirmed using a coimmunoprecipitation assay combined with dithiobis(succinimidylpropionate) (Pierce) cross-linking (1). For this, plasmids encoding FLAG-tagged TBC1D20 and NS5A were cotransfected into human hepatoma cells (Huh7); 24 h after transfections, the cells were incubated at 16°C for 90 min to slow intracellular transport. The cells were then washed twice with phosphate-buffered saline (PBS), overlaid with 1.5 ml PBS containing 600 μM dithiobis(succinimidylpropionate), and incubated on ice for 30 min. After removal of the reactant solution, the reaction was quenched with two 2 ml Tris-buffered saline (40 mM Tris-HCl [pH 8], 150 mM NaCl) incubations for 3 min.

The cells were lysed in 500 μl of IP buffer (10 mM HEPES, pH 7.4, 10 mM NaCl, 0.1% Triton, 1 mM EGTA, Complete mini protease inhibitor tablets [Roche]). Precleared lysates of the cells were immunoprecipitated with either a polyclonal rabbit anti-Flag antibody (Sigma) or a mouse monoclonal anti-NS5A antibody (Virostat) and immobilized protein A/G beads (Pierce). The IP pellets were then washed four times with IP buffer and analyzed by Western blots probed with the reciprocal antibodies.

For IPs involving in vitro translation reactions, NS5A-Flag or NS5AmAH-Flag were in vitro translated (TNT; Promega) in the presence of [^{35}S]methionine (GE Healthcare), and TBC1D20-HA was in vitro translated in the presence of cold methionine. The reactions were stopped by adding cycloheximide, and then equal amounts of extract were mixed and incubated at 30°C for an additional 30 min. HA-TBC1D20 was immunoprecipitated using an anti-HA antibody. The amount of labeled NS5A was determined by sodium dodecyl sulfate-polyacrylamide gel electrophoresis (SDS-PAGE) analysis, followed by fluorography and exposure to X-ray film.

Western blots. Lysates were separated on 10% SDS-PAGE gels and transferred to nitrocellulose membranes using a semidry transfer apparatus, essentially as described previously (17). Membranes were probed with primary antibodies to either NS5A (Virostat; 1:1,000), Flag (Sigma; 1:1,000), GFP (Molecular Probes; 1:1,000), or actin (Sigma; 1:5,000), followed by a corresponding pair of Alexa Fluor 680-coupled (Molecular Probes) and IRDye 800CW-coupled (Rockland Inc.) secondary antibodies. Proteins were visualized with a LI-COR infrared imager (Odyssey), and the images were processed with Odyssey version 1.2 infrared imaging software.

Immunofluorescence assays. Cells expressing GFP and DsRed fusion proteins were fixed with 4% formaldehyde 24 h posttransfection and mounted using a Mowiol mounting medium. Fluorescence images were captured using a Nikon E600 fluorescence microscope equipped with a SPOT digital camera or a Bio-Rad confocal microscope and OpenLab (Improvision, Lexington, MA) image acquisition software.

siRNAs. All small interfering RNAs (siRNAs) were purchased from Dharmacon as duplexes. The sequences of the siRNAs designed against TBC1D20 were as follows: siRNA3, 5′-CCAGCAGAGGCCUGAUAUGUU-3′ and (antisense) 5′-CAUAUCAGGCCUCUGCUGGUU-3′, and siRNA1, 5′-AAGAUACACC AGGCUCUGAAC-3′ and (antisense) 5′-GUUCAGAGCCUGGUGUAUCU U-3′. siGLO, a nontargeting control siRNA labeled with Cy3, served as a negative control and allowed the monitoring of transfection efficiency. An ON-TARGETplus SMARTpool (siCLTC) was used to silence clathrin heavy chain (Dharmacon; L-004001-00). si*CONTROL* Non-Targeting siRNA no. 1 (Dharmacon; D-001210-01-05) was used as a negative control in the real-time PCR experiments. siRNA transfections were done using 100 nM siRNA and Lipofectamine 2000, and siRNA electroporations employed 150 nM siRNA.

Real-time PCR. For real-time PCR experiments, 6×10^6 FLRP1 cells (Huh7 cells harboring a full-length replicon of genotype 1b) (4) were transfected with si*CONTROL* or siRNA3. Twenty-four hours after transfections, the cells were trypsinized, 2×10^5 cells were harvested for the first time point, and the remaining cells were plated in 12-well plates (2×10^5 cells/well). For each time point, RNA was extracted from each of three wells, using 0.5 ml of TRIzol Reagent (Invitrogen) per well according to the manufacturer's directions, and then subjected to reverse transcription using random hexamers and Superscript II reverse transcriptase (Invitrogen, Carlsbad, CA). Real-time PCR was performed on the resulting cDNA to quantify the amounts of TBC1D20, HCV, and actin RNA (in separate reactions) in each sample. Standards were made using an in vitro-transcribed HCV RNA and human actin standard (Applied Biosystems, Foster City, CA). HCV was quantified using primers AGAGCCATAGTGGTCT and CCAAATCTCCAGGCATT GAGC and probe 6-carboxyfluorescein-CACCGGAATTGCCAGGACGAC CGG-6-carboxytetramethylrhodamine. Actin was quantified using beta-actin control reagents (Applied Biosystems) according to the manufacturer's instructions. TBC1D20 was quantified using a TaqMan Gene Expression Assay probe and primer set for TBC1D20 (Applied Biosystems; Hs00299060_m1).

In-cell Western blots. Huh7.5 cells were transfected with either anti-TBC1D20 siRNA duplexes (siRNA3 and siRNA1), siGLO used as a negative control, or siRNA targeting the heavy chain of clathrin (siCLTC) as a positive control. Twenty-four hours after the transfections, the cells were trypsinized, and 20,000 cells were plated per well in a 24-well plate. Forty-eight hours after transfection, the cells were infected with cell culture-grown HCV (titered at a 50% tissue culture infective dose of 3.2×10^4/ml and subsequently concentrated 100-fold prior to inoculation, as described by Lindenbach et al. and Reed and Muench [14, 24]). Adapted from the method of Counihan et al. (7), 6 days after infection, the cells were fixed with 4% formaldehyde and stained with a monoclonal antibody against HCV core protein (17) and a rabbit polyclonal anti-calnexin antibody (Stressgen), followed by the matching secondary goat anti-mouse IRDye800 (Rockland Immunochemicals) or goat anti-rabbit Alexa Fluor 680 (Molecular Probes) antibody. The plates were scanned using an Odyssey infrared imaging system (Li-Cor Biosciences) at a resolution of 169 μm and a laser intensity of 5. The integrative intensities of the signals in each channel were measured using Odyssey version 1.2 infrared imaging software, allowing the determination of the core-to-calnexin normalized signal. In untreated cells, typically over 50% of the cells were infected.

Colony formation assays. In vitro-transcribed RNAs were electroporated into Huh-7 cells, essentially as described previously (10) with minor modifications. Briefly, 100 ng of in vitro-transcribed RNA and 150 nM of siRNA were mixed with 4×10^6 cells in RNase-free PBS (Biowhittaker) and transferred into a 2-mm-diameter gap cuvette (BTX, San Diego, Calif.). Electroporation was performed using a BTX model 830 electroporator (the electroporation conditions were 0.68 kV and five periods of 99 μs at 500-ms intervals). The pulsed cells were left to recover for 10 min at room temperature and then diluted in 10 ml of prewarmed growth medium. The cells were plated in 10-cm tissue culture dishes at different dilutions. The greatest number of cells plated was 3.2×10^6 cells/dish. At 24 h postelectroporation, the cells were supplemented with untransfected feeder Huh-7 cells to a final density of 10^6 cells/plate. Twenty-four hours later, the medium was supplemented with G418 to a final concentration of 1 mg/ml. This selection medium was replaced every 4 days for 3 weeks. Following selec-

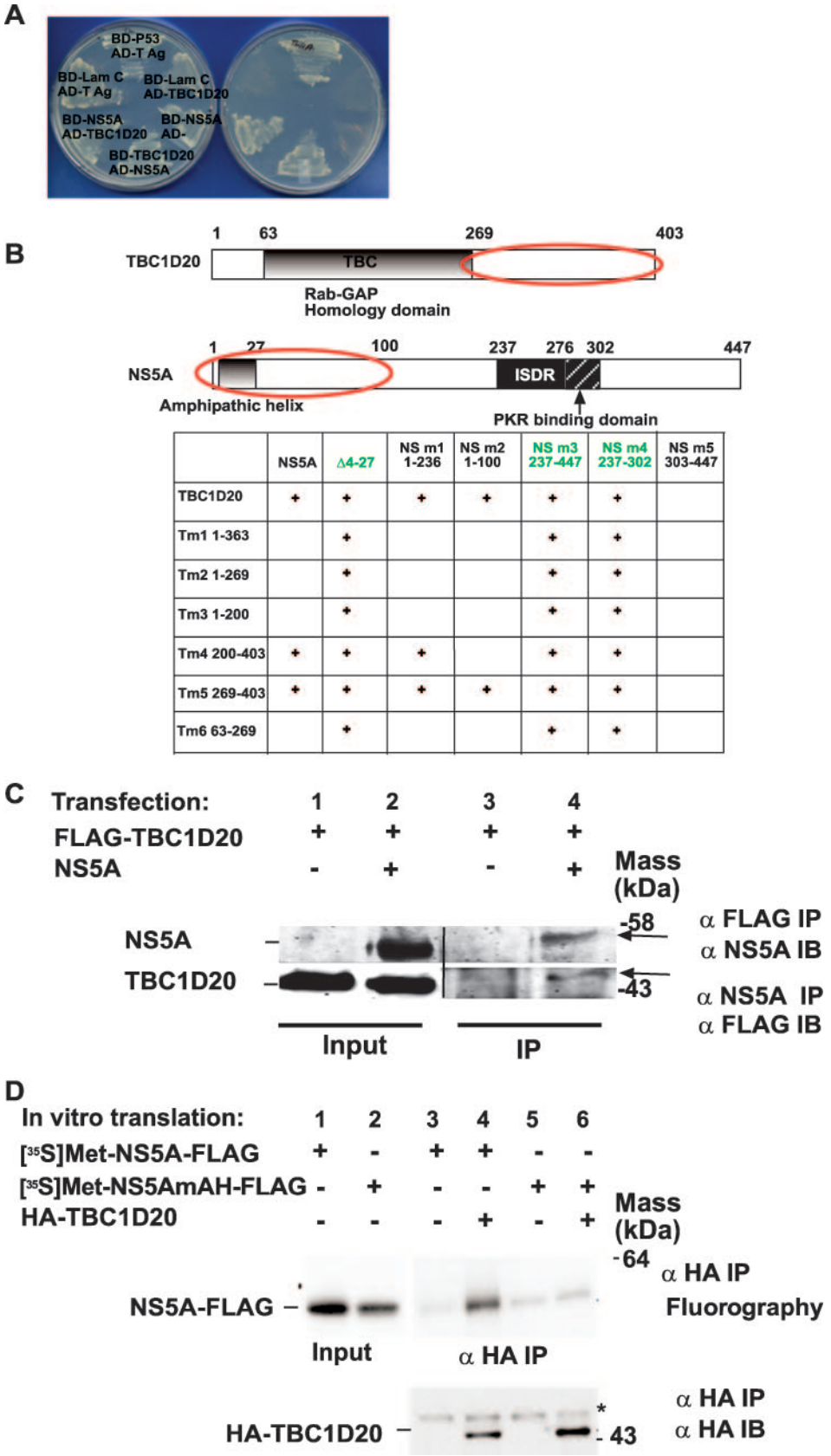

FIG. 1. TBC1D20 interacts with the N terminus of NS5A. (A) (Left) A plate from the GAL4-based yeast two-hybrid assay lacking tryptophan and leucine on which yeast cotransformed with the indicated plasmids was plated, selecting for the presence of both the bait (BD; Leu) and prey

tion, the plates were washed with PBS, incubated in 1% crystal violet in 20% ethanol for 5 min, and washed five times with H_2O to facilitate colony counting.

RESULTS

The Rab-GAP TBC domain protein TBC1D20 is a binding partner protein of NS5A. Full-length NS5A from genotype 1b was used as bait to screen a human liver cDNA prey library in a GAL4-based yeast two-hybrid screen. Out of 8.6×10^5 colonies screened, 73 positive clones were isolated and sequenced. One of these encoded a protein previously termed TBC1D20 (accession number BC014983). TBC1D20 contains a Rab-GAP TBC homology domain found in all known Rab-GAPs (19).

The authenticity of the TBC1D20-NS5A interaction was confirmed in a variety of ways. First, an artifactual false-positive reading due to potential self-activation of either NS5A or TBC1D20 was ruled out by cotransformation with empty prey (for NS5A) or irrelevant bait plasmid (for TBC1D20) (Fig. 1A). Second, prey and bait plasmid inserts were switched to rule out nonspecific interactions (Fig. 1A). To further pinpoint the domains essential for the interaction, a series of deletion mutants of both NS5A and TBC1D20 were prepared. Expression of all mutants was verified using Western blotting (data not shown). Pairs of deletion mutants were then transformed into yeast to test for possible interactions (Fig. 1B). Three of the NS5A mutants (Δ4-27, NS5A 237-447, and NS5A 237-302) grew on selective media without a partner plasmid, indicative of self-activation, and were thus noninformative. Analysis of the remaining clones indicated that the minimal domain sufficient for interaction with TBC1D20 resided within amino acids 1 to 100 of NS5A. Within TBC1D20, the minimal interaction domain with NS5A was mapped to the region containing amino acids 269 to 403.

The TBC1D20-NS5A interaction was further confirmed by reciprocal coimmunoprecipitation assays (Fig. 1C). Lysates from Huh7 cells cotransfected with Flag-tagged TBC1D20 and NS5A were immunoprecipitated with anti-Flag or anti-NS5A antibodies, followed by immunoblotting with either anti-NS5A or anti-Flag, respectively. As shown in the right half of Fig. 1C, TBC1D20 could bring down NS5A and NS5A could bring down TBC1D20, confirming that these proteins interact in cells.

NS5A has an N-terminal AH that is necessary and sufficient for membrane localization and whose genetic disruption impairs HCV replication (5, 10). Our yeast two-hybrid results showed that the TBC1D20-NS5A interaction depends on a region within NS5A that contains the AH. We hypothesized that the AH might play a role in the NS5A-TBC1D20 interaction. For example, the AH could be a part of the epitope necessary for interaction with TBC1D20. Alternatively, the AH might mediate the association of NS5A with the membranes containing TBC1D20 while another domain within the first 100 amino acids of NS5A interacts with TBC1D20. In an attempt to distinguish between these two possibilities, we performed a coimmunoprecipitation experiment using proteins translated in vitro in the absence of membranes. As shown in Fig. 1D, while the wild-type NS5A could be immunoprecipitated with TBC1D20, NS5A with a mutated AH could not. These results further confirm the NS5A-TBC1D20 interaction and suggest that the interaction is mediated by the NS5A AH. Because this AH dependence can be demonstrated in the absence of membranes, the results also suggest that the AH role in the NS5A-TBC1D20 interaction is not limited to simply mediating association with the membranes containing TBC1D20. Rather, an intact AH appears to be required to create the motif for direct interaction with TBC1D20.

Finally, confocal immunofluorescence microscopy demonstrated partial colocalization of the two partner proteins within cells (Fig. 2). Colocalization was detected when fluorescently tagged versions of TBC1D20 and NS5A were expressed in Huh7 cells with in-frame fusions of N-terminal GFP and C-terminal DsRed, respectively (Fig. 2A). Partial colocalization was also detected when GFP-tagged TBC1D20 was transfected into FLRP1 cells (3) (Fig. 2B) or Bart-HA cells (Huh7 cells harboring a subgenomic 1b replicon with an HA tag inserted in frame into the C-terminal segment of NS5A) (Fig. 2C). The fraction of colocalizing NS5A and TBC1D20 could be increased when intracellular transport was inhibited by incubation of the cells for 90 min at 16°C (26) (Fig. 2C).

siRNA-mediated depletion of TBC1D20 inhibits HCV RNA accumulation in full-length replicon cells. We next wished to examine whether HCV replication is dependent on TBC1D20. For this, we turned to siRNA technology to establish a means of inhibiting the level of TBC1D20 in cells. Two custom siRNA duplexes (siRNA3 and siRNA1) were designed against TBC1D20 and tested for efficacy at reducing expression of a GFP-TBC1D20 fusion protein expressed from a plasmid trans-

(AD; Trp) plasmids. LamC, lamin C; T Ag, T antigen. (Right) The same yeast cotransformants, but on a selection plate lacking histidine and adenine, as well as tryptophan and leucine, thus selecting for a reconstituted transcription factor (BD plus AD) mediated by interaction between proteins fused to the respective BD and AD and leading to production of histidine and adenine. This plate demonstrates the specificity of the interaction between NS5A and TBC1D20 and the absence of self-activation with either partner protein alone. See Materials and Methods for additional details. (B) Minimal domains mediating interaction between NS5A and TBC1D20 (circled in red), as determined by interactions of the indicated deletion mutants (the numbers represent the amino acids present in the respective mutants) in yeast two-hybrid assays. +, growth on selective media; green font, noninformative assays due to self-activation of certain mutants. (C) Coimmunoprecipitation of FLAG-tagged TBC1D20 and NS5A from Huh7 cells. Lysates from Huh7 cells cotransfected with FLAG-tagged TBC1D20 and NS5A were immunoprecipitated with anti-FLAG or anti-NS5A antibody, followed by immunoblotting with either anti-NS5A or anti-Flag, respectively. (D) An in vitro-translated AH mutant of NS5A does not interact with TBC1D20. NS5A-FLAG and its AH mutant were in vitro translated in the presence of [^{35}S]methionine. The proteins were then mixed with cold in vitro-translated HA-TBC1D20 and incubated for an additional 30 min at 30°C. HA-TBC1D20 was then immunoprecipitated using an anti-HA antibody. The amounts of labeled wild-type or mutant NS5A were determined by SDS-PAGE analysis, followed by fluorography and exposure to X-ray film. Note that the wild-type, but not AH mutant, NS5A coimmunoprecipitated with TBC1D20 (compare lane 4 to lane 6).

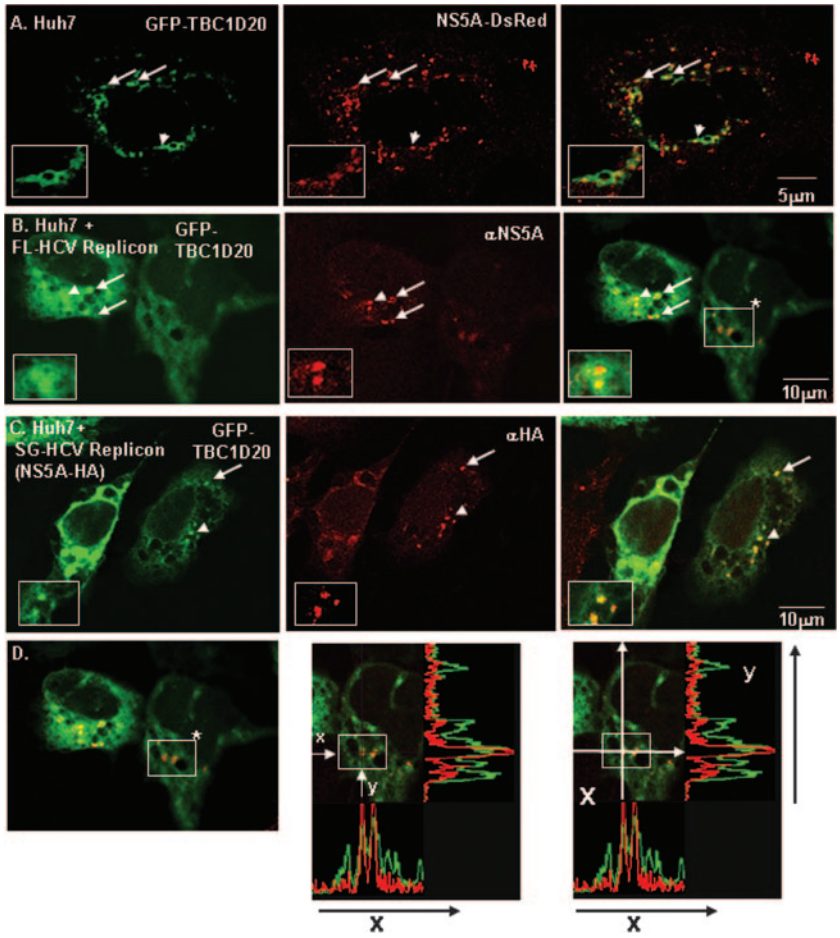

FIG. 2. Partial colocalization of TBC1D20 and HCV NS5A. (A) Plasmids encoding GFP-fused TBC1D20 and NS5A fused to Ds-Red were cotransfected into Huh7 cells. The cells were fixed 24 h after transfection. (B) Colocalization of TBC1D20 and NS5A in full-length replicon cells. A plasmid encoding GFP-fused TBC1D20 was transfected into FLRP1 cells. The cells were fixed after 24 h and stained with anti-NS5A primary and Alexa 594 secondary antibodies. (C) Colocalization of TBC1D20 and NS5A in replicon cells increases under low-temperature transport inhibition. A plasmid encoding GFP-fused TBC1D20 was transfected into cells expressing the Bart-HA replicons (a replication-competent subgenomic replicon with an HA tag inserted into the C-terminal region of NS5A). Twenty-four hours after transfection, the cells were incubated for 90 min at 16°C, followed by immediate fixation. The cells were stained with anti-HA primary and Alexa 594 secondary antibodies. (A to C) Experiments were visualized using a confocal microscope. On the right are merged images of the corresponding left-hand and middle single-channel fluorescent images. Prominent colocalizations are marked with white arrows. The insets in the left lower corners are enlargements of selected colocalized regions (indicated by arrowheads). (D) Representative fluorescence intensities showing colocalization in a cell with low levels of TBC1D20 expression. The left-hand image indicates the areas of colocalization through which line scan intensities were analyzed (note that these are the same colocalizations indicated by the box with an asterisk in the right-hand image of panel B). The middle image indicates the levels of lines scanned (*x* and *y*) to record fluorescence intensities in each of the red and green channels. The right-hand image indicates the actual lines scanned (white lines) with the corresponding fluorescence intensity recordings, which are indicative of colocalization.

fected into the Huh-7 cell line (Fig. 3A). Efficency was determined by Western blotting using anti-GFP antibodies to blot lysates from the above-mentioned cells (Fig. 3B, compare untreated lane 1 to lane 3). siRNA3 reduced most of the GFP signal (Fig. 3A and B) compared to the untreated control, indicating that the siRNA could indeed efficiently knock down TBC1D20 expression. siRNA1 could also inhibit TBC1D20 expression but was somewhat less efficient than siRNA3 (Fig. 3A and B). The efficiency of siRNA3 was also tested against endogenous TBC1D20 in cells harboring stably replicating full-length HCV replicons using a quantitative reverse transcription-PCR assay (Fig. 3C). Endogenous TBC1D20 RNA levels were significantly reduced (65%) within 24 h of siRNA transfection. The highest inhibition levels (more than 80%) were achieved after 72 h.

RNA from the same experiment was tested for HCV RNA levels (Fig. 3D). Viral-RNA levels in TBC1D20 siRNA-treated cells were reduced by 50% 48 h after transfection, reaching a maximum inhibition level of 60% after 96 h. This effect was not seen in the cells transfected with the control siRNA, suggesting a role for TBC1D20 in HCV RNA production. The extent of HCV inhibition as a result of TBC1D20 depletion was equal to or greater than that observed with inhibition of other host targets reported to play a role in HCV replication (29, 35). Of note, TBC1D20 depletion had no obvious effect on cell viability as measured by the Alamar blue assay (Fig. 3E).

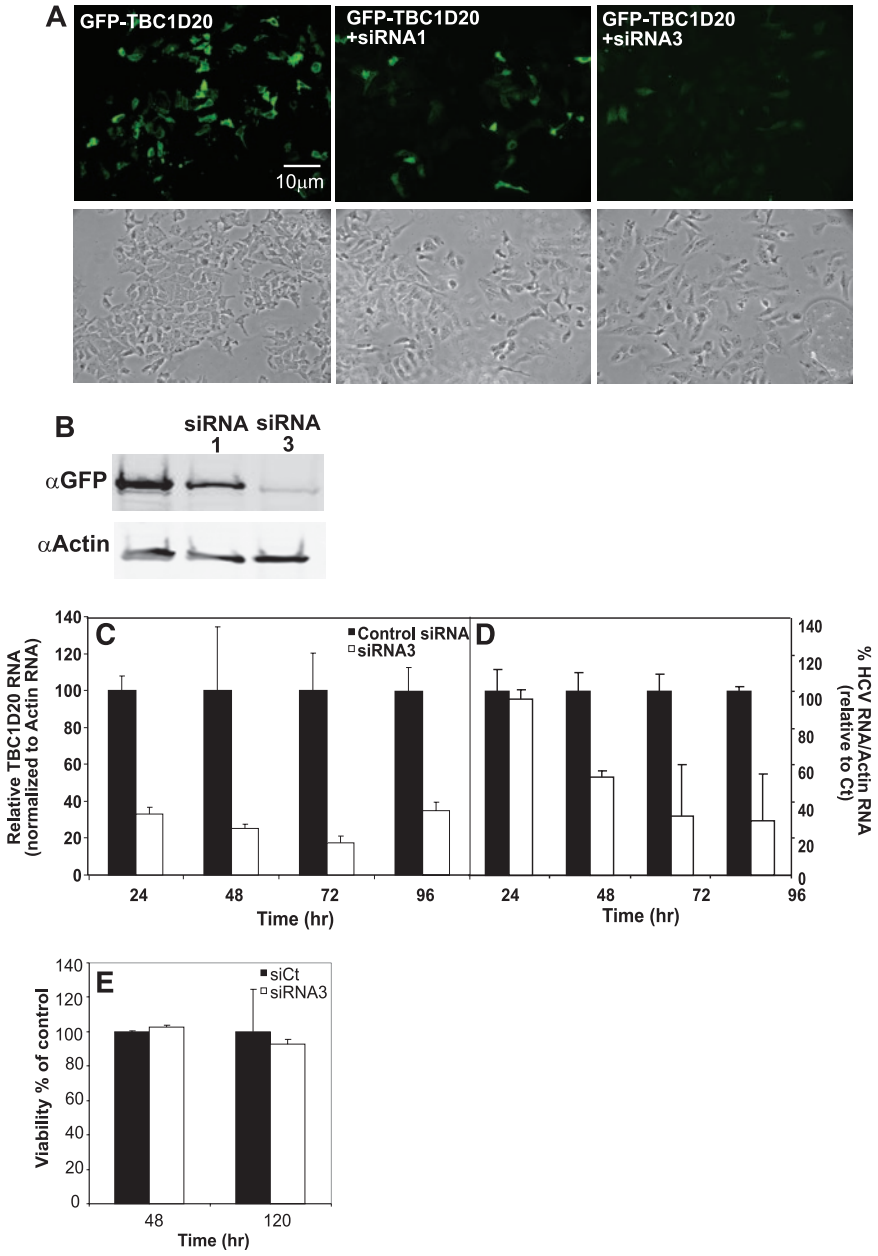

FIG. 3. TBC1D20 knockdown reduces HCV RNA levels in cells with established HCV replication without affecting cell viability. (A) A plasmid encoding a GFP-TBC1D20 fusion protein was transfected into Huh7 cells in the absence (left) or presence (middle and right) of siRNA duplexes (siRNA1 or siRNA3, respectively) designed against TBC1D20. (Top) Images were taken 24 h following transfection using a fluorescence microscope. (Bottom) Corresponding phase-contrast images. (B) Western blots of lysates from cells transfected as in panel A were probed with antibodies against GFP (top) or actin (bottom). (C) TBC1D20 knockdown using custom siRNAs. Cells with established replication of full-length HCV replicons (FLRP1) were transfected with a TBC1D20-targeting siRNA (siRNA3) or a control nontargeting siRNA. Total cellular RNA was harvested every 24 h and was used to determine TBC1D20 mRNA levels by quantitative real-time PCR. (D) RNA from the same experiment was used to determine HCV RNA levels by quantitative real-time PCR. The results were normalized to actin RNA levels. Values (means plus standard deviations) from three independent wells are shown and are expressed as percentages of the control. (E) Alamar blue assays for cell viability were performed at the indicated times following transfection of anti-TBC1D20 (siRNA3) or control (siCt) siRNAs.

Depletion of TBC1D20 inhibits HCV infection and RNA replication. The above-mentioned experiments demonstrated that the efficiency of HCV RNA accumulation is sensitive to TBC1D20 depletion. siRNA-mediated depletion of a target gene, however, is only expected to be maximally efficient over a limited time. Moreover, to the extent that HCV dependence on TBC1D20 is predominantly restricted to the initial establishment of the sites of replication, replication complexes already established prior to anti-TBC1D20 siRNA transfection, or complexes whose effective half-lives are longer than the window of maximal siRNA-mediated TBC1D20 depletion, would not be expected to be significantly affected by our tran-

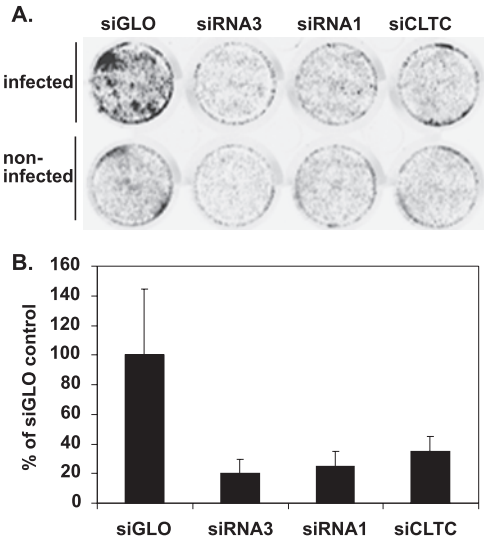

FIG. 4. Depletion of TBC1D20 inhibits HCV infection. (A) In-cell Western blots of Huh7.5 cells transfected with the indicated siRNA duplexes, followed by infection with HCV. Six days after infection, the cells were fixed and stained with a primary antibody against HCV core protein (17) and an IRDye800-conjugated secondary antibody, followed by infrared scanning to identify HCV-infected cells. siGLO, negative control siRNA; siRNA3 and siRNA1, anti-TBC1D20 siRNAs; siCLTC, positive control anti-clathrin heavy chain siRNA. See Materials and Methods for additional details. (B) The above-mentioned infected cells were simultaneously stained with a primary antibody against calnexin- and Alexa Fluor 680-conjugated secondary antibody, and the staining intensity was measured by infrared scanning. The core-to-calnexin normalized signal was quantified and plotted, expressed as a percentage of the control. The data are means plus standard deviations from triplicate wells. Note that depletion of TBC1D20 inhibited infection to the level observed by depletion of clathrin heavy chain (2).

sient depletion of TBC1D20. Thus, siRNA transfection of FLRP cells (as in Fig. 3D) in which HCV replication has already been established may mask the full potential effect of TBC1D20 inhibition on HCV replication. Therefore, we next wished to examine the effect of TBC1D20 depletion on the initial establishment of HCV infection and replication. The ability of TBC1D20 knockdown to prevent new infection was assayed using the recently described infectious HCV clone (14). Target cells were first treated with the above-mentioned siRNAs to deplete endogenous TBC1D20, followed by infection with an inoculum of infectious HCV (genotype 2a, produced in vitro, as described previously [14]). After 6 days, the cells were fixed and processed using a modified in-cell Western assay (7) that employed a monoclonal antibody to the HCV core protein to detect infected cells. As shown in Fig. 4, siRNA3 dramatically reduced the ability of HCV to establish infection compared to cells treated with a control siRNA (siGLO, a fluorescent RISC-free siRNA [Dharmacon]). siRNA1, which was less efficient at depleting TBC1D20 expression, was associated with an intermediate level of HCV inhibition. The extent of inhibition achieved by targeting TBC1D20 was comparable to that achieved by an siRNA targeting the heavy chain of clathrin (siCLTC), which has recently been shown to prevent HCV infection via its inhibition of HCV entry (2). Although there was some variability in the control treatment samples, the inhibition results were clearly significant (siGLO versus siRNA3; t test, $P < 0.02$). We thus conclude that TBC1D20 is required for efficient HCV replication. To further pinpoint the stage of the HCV life cycle dependent on TBC1D20, we performed colony formation assays using high-efficiency second-generation HCV subgenomic replicons (Bart79I [3] carrying the gene for neomycin resistance). These replicons are fully competent for viral-RNA genome replication but lack the viral structural proteins and are unable to either form virus particles or infect new cells. The subgenomic replicons were electroporated into Huh7 cells with siRNA3 (5A, bottom left) or siRNA1 (5A, bottom right) or with siGLO as a negative control (5A, top left). Bart79I with a lethal mutation in the polymerase gene (3) served as a positive control for replication inhibition (5A, top right). The resulting G418-resistant colonies indicative of HCV RNA replication were stained with crystal violet. Again, HCV replication was dramatically inhibited as a result of impairing the expression of TBC1D20.

DISCUSSION

Although positive-strand viruses like HCV replicate their genomes in intimate association with host intracellular membranes and actually create novel membrane structures in order to effect this process, the identities of the requisite proteins provided by the host cell have been largely unexplored. Here, we report the identification of a TBC protein family member, TBC1D20, as a binding partner of the HCV NS5A protein. Like all TBC family members, TBC1D20 contains a Rab-GAP homology domain required for regulating the activity of Rab proteins involved in intracellular vesicular-membrane trafficking. Depletion of TBC1D20 expression severely impairs HCV replication and allows us to propose a model in which TBC1D20 and the Rab-GTPase(s) under its control help mediate the establishment of the membrane-associated HCV replication complex.

We used a yeast two-hybrid screen to isolate this novel cellular binding partner of NS5A. The authenticity of the TBC1D20-NS5A interaction was confirmed using a variety of methods, and mutational analyses allowed the assignment of the respective domains responsible for this interaction. Using different siRNAs specifically synthesized against TBC1D20, we showed that depletion of TBC1D20 dramatically reduced the ability of HCV to establish infection. We identified the membrane-associated replication of the RNA genome as the step impaired by TBC1D20 depletion, as opposed to virus assembly or entry.

Formally, we have shown the requirement for TBC1D20 in two different HCV genotypes. The genotypes we assayed are the ones for which the most efficient replication systems exist. They also span the spectrum of genotypes that are difficult and relatively easy to treat clinically. Thus, we believe it is reasonable to assume our findings are applicable to all genotypes.

Several Rab proteins have been previously implicated in the life cycles of other viruses (human polyomavirus [23], human immunodeficiency virus [32], influenza virus [28], and West Nile and dengue viruses [12]). Most of these reports linked Rab5 and Rab7 to early events of viral infection through inhibition of viral entry using dominant-negative Rab mutants.

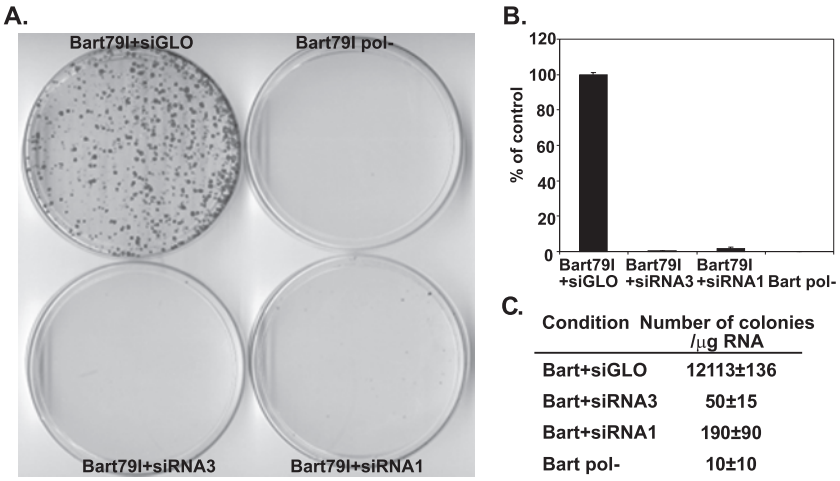

FIG. 5. Depletion of TBC1D20 inhibits HCV RNA replication. (A) Colony formation assays of HCV subgenomic replicons (Bart79I) (3) coelectroporated with anti-TBC1D20 siRNA duplexes (siRNA3, bottom right; siRNA1, bottom left) or with siGLO as a negative control (top left) into Huh-7 cells. The cells were plated in different dilutions. Shown are plates plated with 3.2×10^6 cells. Following selection in G418, resistant colonies were stained with crystal violet. Bart79I with a lethal mutation in the polymerase gene (3) served as a positive control for replication inhibition (top right). For each, a representative plate is shown. (B) Quantitation of the results in panel A, where the number of colonies obtained for each condition is expressed as a percentage of the control. Note that a few colonies were obtained with the siRNA1-treated cells and rare colonies were obtained with the Pol- or siRNA3- treated cells. The error bars indicate standard deviations. (C) Transduction efficiencies expressed as colonies/μg RNA are shown for each condition in panel A.

Others used various immunofluorescence techniques to implicate Rabs in the entry pathways of Semliki Forest virus (33) and mouse polyomavirus (13). One previous report (18) revealed a role for Rab9 in viral replication by depletion of Rab9 expression using siRNA. These studies did not demonstrate, however, any physical interaction between the above-mentioned Rabs and any viral gene products. There is one description of coimmunoprecipitation of Rab5 with rotavirus VP4, but no role for this interaction in the viral life cycle was demonstrated (11). Recently, an interaction between HCV NS4B and Rab5 was described (29), and Rab5 depletion was associated with impaired HCV genome replication. No viral interactions with Rab-GAPs have previously been described. Targeting these Rab master regulators, however, appears to be an effective way to redirect specific components of the host cell trafficking machinery toward viral needs. Our findings show that, indeed, such an attractive opportunity has not been overlooked by HCV.

HCV NS5A has generated considerable interest because it interacts with a variety of host signaling proteins. For example, the highly conserved C-terminal PXXP polyproline motif in NS5A is able to interact with the Src homology 3 domains of the adaptor protein Grb2 (growth factor receptor-bound protein 2) and members of the Src family of tyrosine kinases (16, 30). Several NS5A-interacting proteins have been implicated in protein trafficking and are associated with membrane structures (27, 36). Depletion of some NS5A-interacting partners, such as FBL2 (34), Raf-1 (6), and hVAP-A (35), was shown to affect viral replication. Interestingly, as is presumed for TBC1D20, hVAP-A is involved in intracellular-vesicle trafficking and is thought to be important for establishing the HCV replication complex (31), further highlighting the relationship to, and likely exploitation of, host cell membrane-trafficking machinery for the benefit of the HCV life cycle.

The interaction between HCV NS5A and TBC1D20 is supported by several independent assays, including functional interaction within live cells (Fig. 1A), coimmunoprecipitation (Fig. 1C and D), and colocalization using immunofluorescence (Fig. 2). As with any experiment involving transfection, there is a potential for false-positive interactions induced by high-level overexpression of protein. That the interaction between NS5A and TBC1D20 can be demonstrated in multiple independent systems, including in vitro translation reactions where overexpression of protein is not an issue, argues for the specificity of the NS5A-TBC1D20 interaction. The mutational analysis shown in Fig. 1B identifies the C-terminal domain of TBC1D20 as the region that interacts with NS5A. This fits nicely with the location of the predicted enzymatic domain of TBC1D20, as it appears to leave the TBC domain of TBC1D20 free to interact with the Rab(s) under its control. That TBC1D20 can be efficiently depleted is shown in Fig. 3. Surprisingly, such depletion was not associated with any significant toxicity (Fig. 3E), suggesting that the role of TBC1D20 in host cell trafficking is dispensable, is still functional at low levels of TBC1D20 expression, or can be supplied by other means. However, this does not appear to be the case for the role of TBC1D20 in the HCV life cycle. Indeed, Fig. 4 indicates that TBC1D20 depletion inhibits the establishment of HCV infection. This conclusion is also supported by the colony formation assay data of Fig. 5. Moreover, because this system does not support virus assembly or entry, it helps pinpoint the critical stage of the HCV life cycle that is dependent on TBC1D20. While TBC1D20 might play a role in promoting the translational efficiency of the genomic RNA, because the Rabs regulated by Rab-GAP proteins like TBC1D20 mediate membrane-trafficking events, we favor the hypothesis that TBC1D20 helps mediate the establishment of membrane-associated RNA genome replication.

The precise Rabs that are regulated by individual Rab-GAPs are not known for most TBC domain family members, including TBC1D20. This stems in part from the existence of over 70 Rabs in the human genome. Nevertheless, it will be interesting to identify the specific Rab(s) under the control of TBC1D20, as well as to evaluate the roles of TBC1D20 and other Rab-GAPs in the life cycles of other viruses.

Our study is the first to describe an interaction between a Rab-GAP family member and a viral protein. This highlights a novel mechanism whereby viruses may subvert host cell membrane-trafficking machinery. In the case of HCV, replication occurs on a specialized membrane structure triggered by the virus within the host cell cytoplasm (8). Our results led us to propose a new model in which the establishment and/or maintenance of this membranous replication platform is mediated in part by NS5A's hijacking of TBC1D20 and the Rab-GTPase(s) under its control. Although Rab5 (29) is such a candidate Rab, based on the apparent endoplasmic reticulum localization of TBC1D20 and the postulate that the membrane-associated HCV replication complex is assembled using endoplasmic reticulum-derived membranes containing viral proteins, we predict that the Rab(s) regulated by TBC1D20 is more likely to be one associated with the endoplasmic reticulum. Finally, because inhibition of TBC1D20 severely impaired HCV RNA replication with no obvious effect on cell viability, pharmacologic disruption of TBC1D20, or its interaction with NS5A, can be contemplated as a potential antiviral strategy. Identification of a host cell function upon which the virus depends but whose inhibition the cell can tolerate is particularly attractive in the case of HCV, for which resistance to classic antiviral agents targeting viral functions is expected to be a major challenge in the years to come. Because in a strategy targeting TBC1D20 the targeted locus is a host cell function, i.e., not under genetic control of the virus, it may represent a far greater evolutionary challenge for HCV to overcome than one that could be achieved by simple mutation of its own genome.

ACKNOWLEDGMENTS

We thank Charles Rice for the infectious HCV clone.

This work was supported by a Burroughs Welcome Fund Career Award (to J.S.G.) and RO1-DK064223. E.H.S. is the recipient of an ALF Postdoctoral Research Fellow Award and an Israel Science Foundation Bikura Postdoctoral Fellowship.

REFERENCES

1. **Arnoldi, F., M. Campagna, C. Eichwald, U. Desselberger, and O. R. Burrone.** 2007. Interaction of rotavirus polymerase VP1 with nonstructural protein NSP5 is stronger than that with NSP2. J. Virol. **81:**2128–2137.
2. **Blanchard, E., S. Belouzard, L. Goueslain, T. Wakita, J. Dubuisson, C. Wychowski, and Y. Rouille.** 2006. Hepatitis C virus entry depends on clathrin-mediated endocytosis. J. Virol. **80:**6964–6972.
3. **Blight, K. J., A. A. Kolykhalov, and C. M. Rice.** 2000. Efficient initiation of HCV RNA replication in cell culture. Science **290:**1972–1974.
4. **Blight, K. J., J. A. McKeating, and C. M. Rice.** 2002. Highly permissive cell lines for subgenomic and genomic hepatitis C virus RNA replication. J. Virol. **76:**13001–13014.
5. **Brass, V., E. Bieck, R. Montserret, B. Wolk, J. A. Hellings, H. E. Blum, F. Penin, and D. Moradpour.** 2002. An amino-terminal amphipathic alpha-helix mediates membrane association of the hepatitis C virus nonstructural protein 5A. J. Biol. Chem. **277:**8130–8139.
6. **Burckstummer, T., M. Kriegs, J. Lupberger, E. K. Pauli, S. Schmittel, and E. Hildt.** 2006. Raf-1 kinase associates with hepatitis C virus NS5A and regulates viral replication. FEBS Lett. **580:**575.
7. **Counihan, N. A., L. M. Daniel, J. Chojnacki, and D. A. Anderson.** 2006. Infrared fluorescent immunofocus assay (IR-FIFA) for the quantitation of non-cytopathic and minimally cytopathic viruses. J. Virol. Methods **133:**62–69.
8. **Egger, D., B. Wolk, R. Gosert, L. Bianchi, H. E. Blum, D. Moradpour, and K. Bienz.** 2002. Expression of hepatitis C virus proteins induces distinct membrane alterations including a candidate viral replication complex. J. Virol. **76:**5974–5984.
9. **Einav, S., M. Elazar, T. Danieli, and J. S. Glenn.** 2004. A nucleotide binding motif in hepatitis C virus (HCV) NS4B mediates HCV RNA replication. J. Virol. **78:**11288–11295.
10. **Elazar, M., K. H. Cheong, P. Liu, H. B. Greenberg, C. M. Rice, and J. S. Glenn.** 2003. Amphipathic helix-dependent localization of NS5A mediates hepatitis C virus RNA replication. J. Virol. **77:**6055–6061.
11. **Enouf, V., S. Chwetzoff, G. Trugnan, and J. Cohen.** 2003. Interactions of rotavirus VP4 spike protein with the endosomal protein Rab5 and the prenylated Rab acceptor PRA1. J. Virol. **77:**7041.
12. **Krishnan, M. N., B. Sukumaran, U. Pal, H. Agaisse, J. L. Murray, T. W. Hodge, and E. Fikrig.** 2007. Rab 5 is required for the cellular entry of dengue and West Nile viruses. J. Virol. **81:**4881–4885.
13. **Liebl, D., F. Difato, L. Horníková, P. Mannová, J. Stokrová, and J. Forstová.** 2006. Mouse polyomavirus enters early endosomes, requires their acidic pH for productive infection, and meets transferrin cargo in Rab11-positive endosomes. J. Virol. **80:**4610.
14. **Lindenbach, B. D., M. J. Evans, A. J. Syder, B. Wolk, T. L. Tellinghuisen, C. C. Liu, T. Maruyama, R. O. Hynes, D. R. Burton, J. A. McKeating, and C. M. Rice.** 2005. Complete replication of hepatitis C virus in cell culture. Science **309:**623–626.
15. **Lindenbach, B. D., and C. M. Rice.** 2005. Unravelling hepatitis C virus replication from genome to function. Nature **436:**933–938.
16. **Macdonald, A., K. Crowder, A. Street, C. McCormick, and M. Harris.** 2004. The hepatitis C virus NS5A protein binds to members of the Src family of tyrosine kinases and regulates kinase activity. J. Gen. Virol. **85:**721.
17. **Matto, M., C. M. Rice, B. Aroeti, and J. S. Glenn.** 2004. Hepatitis C virus core protein associates with detergent-resistant membranes distinct from classical plasma membrane rafts. J. Virol. **78:**12047–12053.
18. **Murray, J. L., M. Mavrakis, N. J. McDonald, M. Yilla, J. Sheng, W. J. Bellini, L. Zhao, J. M. Le Doux, M. W. Shaw, C.-C. Luo, J. Lippincott-Schwartz, A. Sanchez, D. H. Rubin, and T. W. Hodge.** 2005. Rab9 GTPase is required for replication of human immunodeficiency virus type 1, filoviruses, and measles virus. J. Virol. **79:**11742.
19. **Pan, X., S. Eathiraj, M. Munson, and D. G. Lambright.** 2006. TBC-domain GAPs for Rab GTPases accelerate GTP hydrolysis by a dual-finger mechanism. Nature **442:**303–306.
20. **Pawlotsky, J.-M.** 2004. Pathophysiology of hepatitis C virus infection and related liver disease. Trends Microbiol. **12:**96–102.
21. **Pawlotsky, J. M.** 1999. Hepatitis C virus (HCV) NS5A protein: role in HCV replication and resistance to interferon-alpha. J. Viral. Hepat. **6**(Suppl. 1)**:** 47–48.
22. **Pfeffer, S., and D. Aivazian.** 2004. Targeting Rab GTPases to distinct membrane compartments. Nat Rev. Mol. Cell. Biol. **5:**886–896.
23. **Querbes, W., B. A. O'Hara, G. Williams, and W. J. Atwood.** 2006. Invasion of host cells by JC virus identifies a novel role for caveolae in endosomal sorting of noncaveolar ligands. J. Virol. **80:**9402.
24. **Reed, L. J., and H. Muench.** 1938. A simple method of estimating 50% endpoints. Am. J. Hyg. **27:**493–497.
25. **Richardson, P. M., and L. I. Zon.** 1995. Molecular cloning of a cDNA with a novel domain present in the tre-2 oncogene and the yeast cell cycle regulators BUB2 and cdc16. Oncogene **11:**1139.
26. **Saraste, J., and E. Kuismanen.** 1984. Pre- and post-Golgi vacuoles operate in the transport of Semliki Forest virus membrane glycoproteins to the cell surface. Cell **38:**535.
27. **Shi, S. T., S. J. Polyak, H. Tu, D. R. Taylor, D. R. Gretch, and M. M. Lai.** 2002. Hepatitis C virus NS5A colocalizes with the core protein on lipid droplets and interacts with apolipoproteins. Virology **292:**198–210.
28. **Sieczkarski, S. B., and G. R. Whittaker.** 2003. Differential requirements of Rab5 and Rab7 for endocytosis of influenza and other enveloped viruses. Traffic **4:**333.
29. **Stone, M., S. Jia, W. Do Heo, T. Meyer, and K. V. Konan.** 2007. Participation of Rab5, an early endosome protein, in hepatitis C virus RNA replication machinery. J. Virol. **81:**4551–4563.
30. **Tan, S. L., H. Nakao, Y. He, S. Vijaysri, P. Neddermann, B. L. Jacobs, B. J. Mayer, and M. G. Katze.** 1999. NS5A, a nonstructural protein of hepatitis C virus, binds growth factor receptor-bound protein 2 adaptor protein in a Src homology 3 domain/ligand-dependent manner and perturbs mitogenic signaling. Proc. Natl. Acad. Sci. USA **96:**5533.
31. **Tu, H., L. Gao, S. T. Shi, D. R. Taylor, T. Yang, A. K. Mircheff, Y. Wen, A. E. Gorbalenya, S. B. Hwang, and M. M. Lai.** 1999. Hepatitis C virus RNA polymerase and NS5A complex with a SNARE-like protein. Virology **263:** 30–41.
32. **Vidricaire, G., and M. J. Tremblay.** 2005. Rab5 and Rab7, but Not ARF6, govern the early events of HIV-1 infection in polarized human placental cells. J. Immunol. **175:**6517–6530.

33. **Vonderheit, A., and A. Helenius.** 2005. Rab7 associates with early endosomes to mediate sorting and transport of Semliki Forest virus to late endosomes. PLoS Biol. **3:**1225–1238.
34. **Wang, C., M. Gale, B. C. Keller, H. Huang, M. S. Brown, J. L. Goldstein, and J. Ye.** 2005. Identification of FBL2 as a geranylgeranylated cellular protein required for hepatitis C virus RNA replication. Mol. Cell **18:**425.
35. **Xue, Q., H. Ding, M. Liu, P. Zhao, J. Gao, H. Ren, Y. Liu, and Z. T. Qi.** 2007. Inhibition of hepatitis C virus replication and expression by small interfering RNA targeting host cellular genes. Arch. Virol. **152:**955.
36. **Zech, B., A. Kurtenbach, N. Krieger, D. Strand, S. Blencke, M. Morbitzer, K. Salassidis, M. Cotten, J. Wissing, S. Obert, R. Bartenschlager, T. Herget, and H. Daub.** 2003. Identification and characterization of amphiphysin II as a novel cellular interaction partner of the hepatitis C virus NS5A protein. J. Gen. Virol. **84:**555–560.